

Solvothermal synthesis of nanosized cobalt antimonide for thermoelectrics

Nidhi Puri¹, Raj K. Gupta¹, Akhyaya K. Pattanaik², Navin C. Mehra³, Ajit K. Mahapatro^{1,*}, Ram P. Tandon^{1,†}

¹Department of Physics and Astrophysics, University of Delhi, Delhi 110007, India

²Department of Physics, Veer Surendra Sai University of Technology, Burla, Orissa, 768018, India

³Department of Geology, University of Delhi, Delhi 10007, India

*Corresponding author

DOI: 10.5185/amp.2018/846

www.vbripress.com/amp

Abstract

The present paper highlights the synthesis of cobalt antimonide (CoSb₃) micro/nanostructures by following solvothermal technique with water as solvent. Recipe is optimized for preparation of refined CoSb₃ compounds and demonstrated that a high processing temperature of 500 °C and long duration of 72 hr indicates presence of CoSb₃ phase. The microstructures and composition of the as synthesized CoSb₃ nanocomposites are characterized to achieve the optimized phase. The morphologies as imaged using field emission scanning electron microscope resemble granules for the as-synthesized CoSb₃. The phase purity and crystallographic structure of the as-synthesized CoSb₃ nanocomposites as determined by XRD indicates the formation of the cubic phase of CoSb₃ and agrees well with the JCPDS data mentioned for the highly pure CoSb₃. The EDX estimates the elemental composition of Co and Sb in 1:3 stoichiometric ratio for the as-synthesized CoSb₃. The currently prepared nanosized skutterudite CoSb₃ material synthesized by solvothermal method could be utilized as active material for the development of highly efficient thermoelectric devices. Copyright © 2018 VBRI Press.

Keywords: Cobalt antimonide, solvothermal synthesis, thermoelectric materials.

Introduction

The nanosized cobalt antimonide (CoSb₃) based skutterudites are among the most prospective thermoelectric (TE) materials activated at the intermediate temperature range (300°C to 550°C) for suitable utilization in generating thermopower. The advantages including, high performance, low cost, and accessibility in tailoring the thermal and electrical transport through structural engineering, insists utilization of CoSb₃ as a potential material for the next generation thermoelectrics. Among the TE materials investigated [1], the family of skutterudite crystal structures provide promising semiconducting properties and have attracted much attention for showing high performance in typical “phonon-glass-electron crystals” (PGEC) [2, 3] that possess electronic properties of a good semiconductor single crystal and thermal properties akin to the amorphous materials, i.e., poor thermal conductor and good electrical conductor. CoSb₃ provides a binary skutterudite structure that has a formula of MX₃ (Im3), where M is a transition metal atom (Co, Rh, or Ir) and X is a pnictogen atom (P, As, or Sb), and is characterized as cubic crystalline structure containing large cages and four-membered planar rings of X. Binary skutterudites have superior $S^2\sigma$ due to their appropriate band gaps and high carrier mobilities. The higher thermal conductivities

in these materials hinder their applications for fabricating efficient TE devices [4]. According to the concept of “phonon-glass-electron-crystal,” [5, 6] it is possible to reduce the thermal conductivity of CoSb₃ by introducing impurities that could fill the voids in the CoSb₃ structure and forms partially filled skutterudites. Here, the filler atoms rattle inside the oversized cages and acting as the additional phonon scattering centers, thus reducing the lattice thermal conductivity [7-9]. CoSb₃ is a narrow band gap semiconductor (0.25 eV) [10] with body-centered cubic crystal structure having a space group of Im3, contains elements with low-electronegativity difference and high degree of covalent bonding enabling high carrier mobilities, and exhibits good electron-crystal properties [11].

CoSb₃ skutterudite materials are generally processed by mechanical alloying [11], ball milling [11], arc melting [12], chemical alloying [13], solid-state reaction [14], ultrasonic spray pyrolysis [15], co-precipitation [13], sol-gel [16], and solvothermal methods [17, 18]. However, the solvothermal method is a simple and effective way for the synthesis of nanostructured materials and has advantages such as its relatively low processing temperature, high reproducibility, low cost, large-scale production, and its ability to control the size and morphology of the material [17, 18]. The present work reports an attempt for synthesization of CoSb₃

micro/nano-structures, suitable for thermoelectric applications following a recipe of cost effective solvothermal method. The effect of annealing on the purity of crystalline structure of the as-synthesized CoSb_3 is monitored using the X-ray diffraction (XRD), the composition using electron dispersive X-ray spectroscopy (EDX) and the morphological studies have been imaged using the field emission scanning electron microscope (FESEM), and transmission electron microscope (TEM).

Experimental details

Materials/ Chemicals

All chemicals used in this work are procured from the Sigma Aldrich Co., USA. In the present work, cobalt (II) chloride hexahydrate ($\text{CoCl}_2 \cdot 6\text{H}_2\text{O}$), antimony (III) chloride (SbCl_3), sodium borohydride (NaBH_4), ethylene diamine tetra acetic acid (EDTA), and sodium hydroxide (NaOH) were used as the precursors for the synthesis of CoSb_3 nanocomposites.

Material synthesis/ Reactions

Nanocomposites of CoSb_3 are synthesized following the solvothermal process and stepwise recipe is schematically drawn in **Scheme 1**. Analytically pure $\text{CoCl}_2 \cdot 6\text{H}_2\text{O}$ and SbCl_3 , in a molar ratio of 1:3 are used as starting materials by placing in a beaker containing 500ml of distilled water ($\text{DI-H}_2\text{O}$). A sufficient amount of NaBH_4 as reducing agent and 8g of NaOH is added into the beaker. The beaker is heated to 500°C on a hot plate and stirred continuously using a magnetic stirrer. The reflux reaction is carried out for 72 hrs. After the reaction, the beaker is cooled naturally to room temperature. The black precipitate is collected, rinsed with $\text{DI-H}_2\text{O}$ and ethanol for several times, and the resulting precipitate is dried in an oven at 80°C , to obtain the as-synthesized CoSb_3 in solid form.

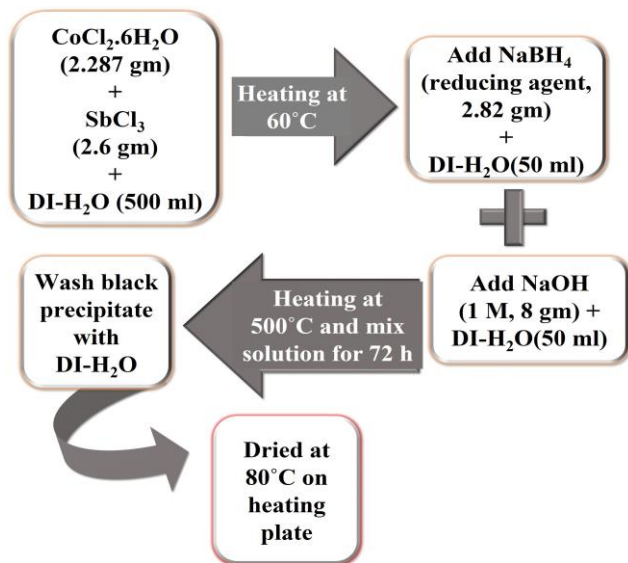


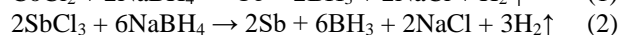
Fig. 1. Schematics of the chemical recipe followed for preparation of CoSb_3 nanocomposites.

Characterizations

The surface morphology of the as-synthesized samples are imaged using the field emission scanning electron microscope (FESEM; Jeol JSM 6610LV). Powder X-ray diffraction (XRD) patterns were collected in the 2θ range of, 20° – 80° of the as-synthesized and annealed CoSb_3 nanocomposites using X-ray diffractometer (XRD; Bruker D8 Discover). The elemental analysis of the CoSb_3 is studied using an energy-dispersive analysis of X-rays (EDAX, Jeol JSM 6610LV). Transmission electron microscopy (TEM) images were obtained on a Tecnai G2 UT 30, with an accelerating voltage of 300 kV.

Results and discussion

The chemical reactions for synthesis of CoSb_3 is written as:



The above reaction mechanism indicates the stepwise formation of the CoSb_3 phase. In the beginning of the reaction process, the strong reducing agent NaBH_4 rapidly and completely reduces the Co^{2+} and Sb^{3+} ions to Co and Sb atoms, as indicated by the reaction equations (1) and (2), respectively, and combine at high processing temperatures and duration for chemical reaction to form the skutterudite, CoSb_3 .

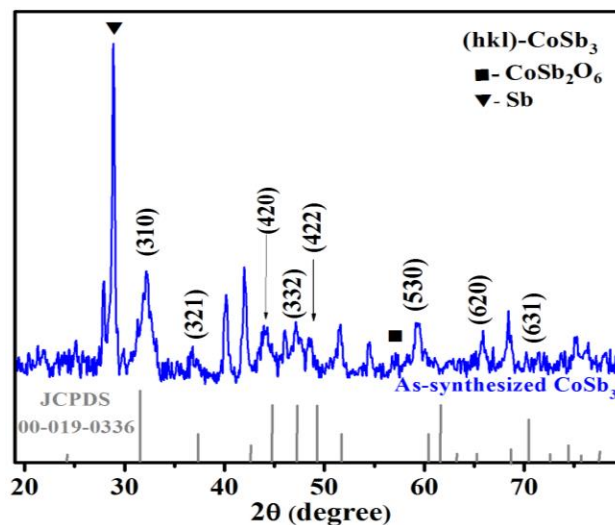


Fig. 2. XRD pattern for the as-synthesized CoSb_3 (blue). The lines at the bottom are the various planes assigned for pure CoSb_3 , as mentioned in JCPDS No. 00-019-0036.

The XRD spectra for the as-synthesized CoSb_3 samples prepared solvothermally is shown in **Fig. 2**, indicating a dominant peak for Sb, which is an intermediate product with small peaks for skutterudite phase CoSb_3 which can be attributed to the low processing temperature or short duration for the synthesis. The earlier work suggests that a synthesis temperature of around 250°C with long reaction duration is necessary for

obtaining pure phase of CoSb_3 without the impurities Sb and CoSb_2 and the impurities will be formed at low processing temperature and short duration [17]. The XRD patterns for post-annealed samples exhibits diffraction peaks corresponding to the skutterudite crystal structure of CoSb_3 . In addition, the absence of the intermediate product containing Sb is observed except for a trace of CoSb_2 and the presence of small amount of oxides. It can be ascribed that during the annealing process, the residual element of Sb starts reconstructing to form CoSb_2 and CoSb_3 phases in the vacuum ampoule, leading to reduction in the amount of elemental Sb compared to the as-synthesized CoSb_3 nanocomposites. The diffraction peaks located for (310), (321), (420), (332), (422), (530), (620), and (631) in all the XRD spectra can be indexed as binary skutterudite CoSb_3 with cubic phase, space group $\text{Im}\bar{3}$ and agrees with the standard XRD profile authenticated among the scientific community (JCPDS File: 000-019-0336) of the cubic CoSb_3 .

Fig. 3. shows the morphologies of the as-synthesized and post-annealed CoSb_3 nanocomposites, respectively, as imaged through the FESEM. The as-synthesized CoSb_3 indicates nanocomposites comprising of granules with agglomerated clusters of near-spherical nanoparticles in 20-30 nm dimensions. The EDX measurements, as represented in **Fig. 4**, recodes the contents of elemental Co and Sb in both the as-synthesized and annealed nanocrystals with reduced contents of Sb for the annealed samples. The table in the inset of **Fig. 3b** shows the composition of the elemental Co and Sb contents present in the as-synthesized and post-annealed CoSb_3 nanocomposites, confirming the stoichiometric ratio of 1:3 for the as-synthesized and post-annealed CoSb_3 samples. The presence of the Cu peak in the EDX spectra is the content of the supporting TEM grid. The initial combined analysis of the FESEM and EDX indicates that the regular features of relatively larger sizes in annealed samples indicate formation of larger crystalline structures originated by removal of elemental Sb from the as-synthesized samples.

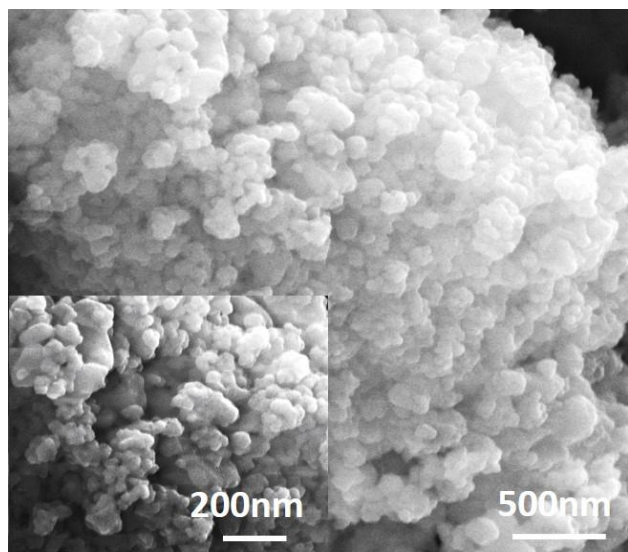


Fig. 3. FESEM images for the as-synthesized CoSb_3

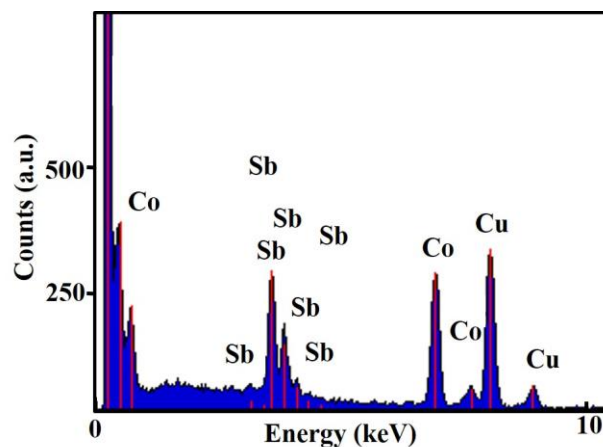


Fig. 4. Energy dispersive X-ray (EDX) spectroscopy for as-synthesized CoSb_3 and shows the composition of the elemental Co and Sb content present in the as-synthesized CoSb_3 nanocomposites.

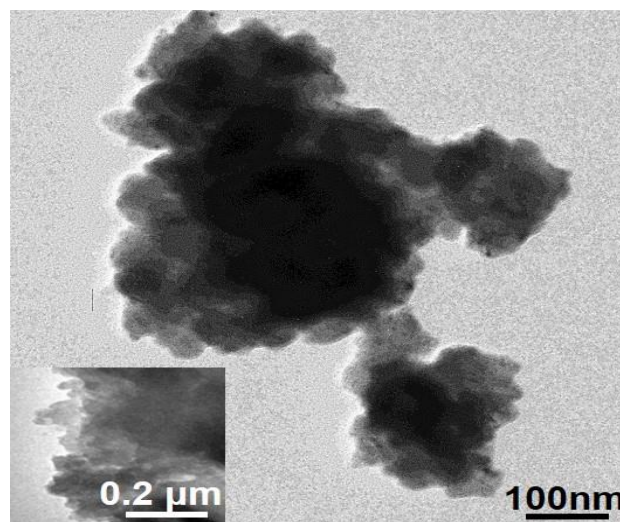


Fig. 5. TEM image of the as-synthesized CoSb_3 nanocomposites.

The **Fig. 5** represents the TEM image of the as-synthesized CoSb_3 indicating clusters of irregular granule like nanostructure particles of dimensions 10-20 nm with uniform size distribution. The observed crystallographic structure for the CoSb_3 based skutterudites have the potential to possess a large unit cell, heavy constituent atoms with low electronegativity differences, and high carrier mobility [19], as expected for a good thermoelectric material.

Conclusion

A solvothermal recipe for synthesization of micro/nano-structured CoSb_3 skutterudites has been demonstrated, with $\text{CoCl}_2 \cdot 6\text{H}_2\text{O}$ and SbCl_3 as precursors and NaBH_4 as reductant. NaBH_4 played a key role in the formation of cobalt antimonide because of its energy supply and strong reduction effect. X-ray-diffraction indicates single-phased CoSb_3 is achieved for the present solvothermal synthesis, and recipe is refined to remove the elemental Sb that is generally present in the final CoSb_3 as residue. The as-prepared CoSb_3 powders were composed of irregular

shaped granular nanoparticles (20-30 nm) agglomerated with a uniform size distribution of about 100-400 nm as observed in microstructural analysis. The solvothermal synthesis of nanosized CoSb₃ provides a profitable way to develop novel nanostructured skutterudite based thermoelectric materials.

Acknowledgements

The authors would like to thank the Defence Research and Development Organization (DRDO), India, and the Research and Development Grant of the University of Delhi, Delhi, India, for providing the financial support to pursue the research work. AKP would like to thank the Academy of Science, Bangalore, for providing opportunity to work in this research through the Summer Fellowship 2015.

Author's contributions

Conceived the plan: RPT, AKM, NP; Performed the experiments: NP, RKG, AKP; Data analysis: NP, AKM; Wrote the paper: NP, AKM. Authors have no competing financial interests.

References

1. Javier Garc a-Mart nez, Nanotechnology for the Energy Challenge, John Wiley & Sons, **2013**.
DOI: [10.1016/j.nanoen.2012.09.012](https://doi.org/10.1016/j.nanoen.2012.09.012)
2. Sales, B. C.; Mandys, D.; Chakoumakos, B. C.; Keppens, V.; Thompson, J. R.; *Phys. Rev. B*, **1997**, 56, 15081.
DOI: [10.1103/PhysRevB.56.15081](https://doi.org/10.1103/PhysRevB.56.15081)
3. Nolas, G. S.; Morelli, D. T.; Tritt, T.M.; *Annu. Rev. Mater. Sci.*, **1999**, 29, 89.
DOI: [10.1146/annurev.matsci.29.1.89](https://doi.org/10.1146/annurev.matsci.29.1.89)
4. Li, J.; Liu, W.; Zhao, L. D.; and Zhou, M.; *NPG Asia Materials*, **2010**, 2, 152–158.
DOI: [10.1038/asiamat.2010.138](https://doi.org/10.1038/asiamat.2010.138)
5. Slack, G. A. In *Thermoelectric Handbook*; Powe, D. M., Ed.; CRC: Boca Raton, FL, **1995**, p 407.
6. Slack, G. A.; Tsoukala, V. G.; *J. Appl. Phys.* **1994**, 76, 1665.
DOI: [10.1063/1.357750](https://doi.org/10.1063/1.357750)
7. Tritt, T. M.; Nolas, G. S.; Slack, G. A.; Ehrlich, A. C.; Gillespie, D. J.; and Cohn, J. L.; *J. Appl. Phys.* **1996**, 79, 8412.
DOI: [10.1063/1.362515](https://doi.org/10.1063/1.362515)
8. Meisner, G. P.; Morelli, D. T.; Hu, S.; Yang, J.; Uher, C.; *Phys. Rev. Lett.* **1998**, 80, 3551.
DOI: [10.1103/PhysRevLett.80.3551](https://doi.org/10.1103/PhysRevLett.80.3551)
9. Singh, D. J.; Pickett, W. E.; *Phys. Rev. B*, **1994**, 50, 11235-11238.
DOI: [10.1103/PhysRevB.50.11235](https://doi.org/10.1103/PhysRevB.50.11235)
10. Kumari, L.; Li, W.; Huang, J. Y.; and Provencio, P. P.; *Nanoscale Res Lett*, **2010**, 5, 1698–1705.
DOI: [10.1007/s11671-010-9700-4](https://doi.org/10.1007/s11671-010-9700-4)
11. Yang, J.; Chen, Y.; Peng, J.; Song, X.; Zhu, W.; Su, J.; Chen, R.; *J. Alloys Compd.*, **2004**, 375, 229.
DOI: [10.1016/j.jallcom.2003.11.036](https://doi.org/10.1016/j.jallcom.2003.11.036)
12. Kawaharada, Y.; Kurosaki, K.; Uno, M.; Yamanaka, S.; *J. Alloys Compd.*, **2001**, 315, 193.
DOI: [10.1016/S0925-8388\(00\)01275-5](https://doi.org/10.1016/S0925-8388(00)01275-5)
13. Wang, M.; Zhang, Y. M.; Muhammed; *Nanostruct. Mater.*, **1999**, 12, 237.
DOI: [10.1016/S0965-9773\(99\)00107-5](https://doi.org/10.1016/S0965-9773(99)00107-5)
14. Chapon, L.; Ravot, D.; Tedenac, J.C.; *J. Alloys Compd.*, **1999**, 282, 58.
DOI: [10.1016/S0925-8388\(98\)00850-0](https://doi.org/10.1016/S0925-8388(98)00850-0)
15. Wojciechowski, K. T.; Morgiel, J.; in *Proceedings of 22nd International Conference on Thermoelectrics*. La Grande Motte, France, August **2003**, pp. 97
16. Chu, Y.; Tang, X.; Zhao, W.; Zhang, Q.; *Cryst. Growth Des.*, **2008**, 8, 208.
DOI: [10.1021/cg060924j](https://doi.org/10.1021/cg060924j)
17. Mi, J. L.; Zhao, X.B.; T.J.; Tu, J.P.; Cao, G. S.; *J. Alloys Compd.*, **2006**, 417, 269.
DOI: [10.1016/j.jallcom.2005.09.033](https://doi.org/10.1016/j.jallcom.2005.09.033)
18. Xie, J.; Zhao, X.B.; Mi, J.L.; Cao, G.S.; Tu, J. P.; *J. Zhejiang Univ. Sci.*, **2004**, 5, 1504.
DOI: [10.1631/jzus.2004.1504](https://doi.org/10.1631/jzus.2004.1504)
19. Chen, Z. G.; Han, G.; Yang, L.; Cheng, L.; and Zou, J.; *Progress in Natural Science: Materials International*, **2012**, 22(6), 535-549.
DOI: [10.1016/j.pnsc.2012.11.011](https://doi.org/10.1016/j.pnsc.2012.11.011)